International Journal of Nanomedicine

Dovepress

open access to scientific and medical research

Open Access Full Text Article

ORIGINAL RESEARCH

Tribological and corrosion behaviors of warm- and hot-rolled Ti-13Nb-13Zr alloys in simulated body fluid conditions

This article was published in the following Dove Press journal:
International Journal of Nanomedicine
1 October 2015
Number of times this article has been viewed

Taekyung Lee[1]
Eshaan Mathew[2]
Santhosh Rajaraman[2]
Geetha Manivasagam[2]
Ashok Kumar Singh[3]
Chong Soo Lee[4]

[1]Department of Mechanical Engineering, Northwestern University, Evanston, IL, USA; [2]Centre for Biomaterials Science and Technology, School for Mechanical and Building Sciences, Vellore Institute of Technology, Vellore, Tamil Nadu, India; [3]Defense Metallurgical Research Laboratory, Hyderabad, India; [4]Graduate Institute of Ferrous Technology (GIFT), Pohang University of Science and Technology (POSTECH), Pohang, Republic of Korea

Correspondence: Geetha Manivasagam
Centre for Biomaterials Science and Technology, School for Mechanical and Building Sciences, Vellore, #201 CDMM Block, Vellore 632-014, TN, India
Email geethamanivasagam@vit.ac.in

Chong Soo Lee
Dean's Office, GIFT, POSTECH, 77 Cheongam-ro, Nam-gu, Pohang 790-784, Gyeongbuk, Republic of Korea
Email cslee@postech.ac.kr

Abstract: Development of submicrocrystalline structure in biomedical alloy such as Ti-13Nb-13Zr (in wt%) through warm-rolling process has been found to enhance mechanical properties compared to conventional thermomechanical processing routes including hot-rolling process. The present study investigated the tribological and corrosion behaviors of warm-rolled (WR) and hot-rolled Ti-13Nb-13Zr alloys which have not been studied to date. Both tribological and corrosion experiments were carried out in simulated body fluid conditions (Hank's solution at 37°C) based on the fact that the investigated alloys would be used in a human body as orthopedic implants. The WR Ti-13Nb-13Zr demonstrated a submicrocrystalline structure that provided a significant enhancement in hardness, strength, and corrosion resistance. Meanwhile, there was no notable difference in wear resistance between the WR and hot-rolled samples despite the different microstructure and hardness. The present study confirmed the enormous potential of WR Ti-13Nb-13Zr with not only great mechanical properties but also high corrosion resistance in the simulated body fluid.

Keywords: titanium alloy, multi-pass caliber-rolling, grain refinement, tribology, corrosion

Introduction

Titanium and its alloys are regarded as one of the most promising materials for orthopedic biomedical implants and are considered as an alternative to conventionally used stainless steel due to their low elastic modulus, low density, higher corrosion resistance, and superior biocompatibility.[1,2] The conventional Ti-6Al-4V alloy, which falls under the category of (α+β) alloy, is extensively used in the fabrication of hip, knee, heart, and spinal implants due to high specific strength and corrosion resistance. Nevertheless, this material has three serious problems.[3] First, it possesses a higher modulus of elasticity (110 GPa) compared to bone tissue (20–30 GPa) leading to stress shielding effect. Second, alloying elements Al and V were reported to have toxicity associated with Alzheimer's disease. Third, a poor wear resistance of titanium and its alloys is another drawback that limits their usage as load-bearing components in the biomedical industry. Moreover, the accumulation of wear debris between tissue and implant induces an adverse cellular response, inflammation, and loosening of implant due to the process called osteolysis.[4,5]

A number of methods have been suggested to enhance biomaterial performances of titanium and its alloys, such as alloy design, powder metallurgy, and thermomechanical process.[6] In particular, the development of β- and near-β-type titanium alloys, such as Ti-Mo, Ti-Nb-Zr, Ti-Mo-Zr-Fe, and Ti-Nb-Zr-Ta systems, are considered as a better alternative as they show a low elastic modulus (45–90 GPa), high corrosion resistance,

submit your manuscript | www.dovepress.com
Dovepress
http://dx.doi.org/10.2147/IJN.S79996

and biocompatibility due to their alloying elements.[7] Some of these alloys have already been approved by American Society for Testing and Materials (ASTM) and/or US Food and Drug Administration (FDA) for an orthopedic implant material.[8] Amongst various β- and near-β-type titanium alloys, Ti-13-Nb-13Zr alloy has been extensively studied in the aspect of thermomechanical processing for implant applications.[9–11] Conventionally Ti-13Nb-13Zr is hot-rolled (HR) above the β-transus temperature, but recent research suggests the potential of warm-rolling performed below the β-transus temperature with improved mechanical properties.[11,12]

Although the mechanical properties were found to be improved by the warm-rolling, until now no investigations have been done on the effect of this process on tribological and corrosion behaviors despite the importance of the topic. High resistance to corrosion is another essential factor for an implant material as the corrosion deteriorates mechanical properties and may lead to periprosthetic bone loss.[5] Thus, the present work aims at clarifying the tribological response and corrosion resistance of Ti-13Nb-13Zr alloy manufactured by the warm- and conventional hot-rolling processes.

Material and methods

ASTM F1713-08 Ti-13Nb-13Zr (in wt%) alloy was prepared in two ways for this study: warm-rolled (WR) or conventionally HR conditions. First, Ti-13Nb-13Zr rods, 28 mm in diameter, were purchased from Hyundai Titanium Co., Incheon, Republic of Korea. They were solution-treated at 800°C for an hour followed by water quenching. The material was then reheated at 650°C for an hour and WR at the same temperature using a multi-pass caliber-rolling process.[11] The reduction of area was calculated to be 90%. Second, Ti-13Nb-13Zr plates were manufactured using the vacuum-arc technique at Defense Metallurgical Research Laboratory, India. The material was melted in the disc shape of 110 mm in diameter and 12 mm thickness in non-consumable vacuum arc furnace using titanium sponge, niobium powder, and zirconium chips. The melting was carried out in copper crucible under the partial pressure of ultra-high purity argon gas. This process was repeated five to six times flipping the disc in order to ensure chemical homogeneity. Afterward, the disc-shaped sample was HR from 800°C to 650°C with a thickness reduction of 63% followed by air cooling.

The microstructural analysis was carried out using scanning electron microscopy (SEM; JSM-6330F, JEOL, Tokyo, Japan) with samples which were chemically etched in Kroll's reagent consisting of 2 mL HF, 2 mL HNO_3, and 96 mL H_2O to reveal the microstructures and wear behaviors. Electron backscatter diffraction (EBSD; Quanta 3D FEG, FEI, Hillsboro, OR, USA) analysis with electropolished samples was conducted to reveal grain and phase structures. The data were analyzed with Orientation Imaging Microscopy Data Analysis (OIM; EDAX Inc., Mahwah, NJ, USA) (eg, the average grain size, *d*). X-ray diffraction (XRD; Bruker XRD D8-Advance, Bruker Corporation, Billerica, MA, USA) analysis was performed at room temperature to confirm phase constituents with 2.2 kW Cu anodes and a scan rate of 0.278°/min.

The hardness was evaluated using a standard Vickers hardness tester with a load of 500 gf and dwell time of 10 seconds with mirror-polished samples. Hank's solution was prepared in laboratory for evaluating the wear behavior. The solution consists of (0.185 g $CaCl_2$ [1.258 mol], 0.4 g KCl [0.00536 mol], 0.06 g KH_2PO_4 [0.0004 mol], 0.1 g $MgCl_2 \cdot 6H_2O$ [0.00049 mol], 0.1 g $MgSO_4 \cdot 7H_2O$ [0.00041 mol], 8.0 g NaCl [0.137 mol], 0.35 g $NaHCO_3$ [0.00417 mol], 0.48 g $Na_2HPO \cdot 12H_2O$ [0.00269 mol], and 1.00 g D $C_6H_{13}NO_5$ HCl [0.004637 mol]). This solution was made up to 1,000 mL with distilled water. The wear test was performed using automated ball-on-plate reciprocating wear tester (TR-285M1, Ducom Instruments, Karnataka, India) with sliding motion against alumina balls of 6 mm diameter. Specimens of 30 mm ×20 mm ×4.5 mm were mechanically polished and ultrasonically cleaned with acetone prior to the experiment. The weight loss was measured with an electronic weighing machine (Adventure Pro AVG 264, Ohaus Corporation, Parsippany, NJ, USA) of 10^{-4} mg of accuracy to evaluate the wear rate.

Corrosion behaviors were investigated in Hank's solution with 10 mm ×10 mm ×4.5 mm specimens using a potentiostat (Gill AC, ACM Instruments, Cumbria, UK). The saturated calomel plate and platinum foil were used as the reference and counter electrodes, respectively. Open-circuit potential test was performed for an hour to achieve a steady potential, and then potentiodynamic polarization test was started from an initial potential of 250 mV below the corrosion potential. The scan rate was 0.166 mV/s as per ASTM F2129 standards. The polarization tests were repeated three times for each specimen for reproducibility of the data.

Results and discussion

Figure 1 presents the SEM and EBSD data of the WR and HR alloys. The micrographs clearly revealed the presence of α and β phases, while martensitic laths were not confirmed. The WR alloy exhibited a significantly fine microstructure oriented along the rolling direction (RD), in which ultrafine

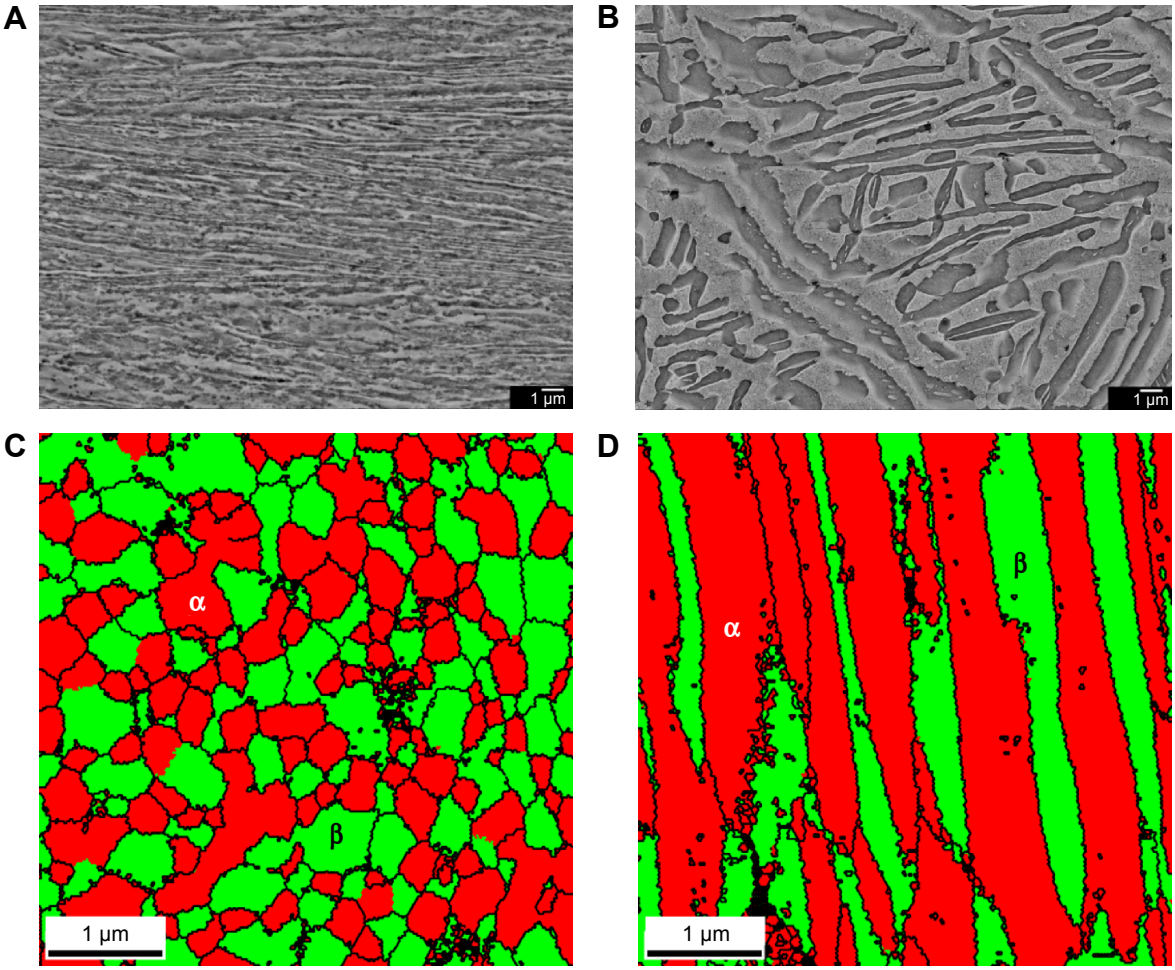

Figure 1 Microstructure of the investigated alloys.
Notes: SEM micrograph of (**A**) WR and (**B**) HR Ti-13Nb-13Zr, and EBSD grain/phase map of (**C**) WR and (**D**) HR Ti-13Nb-13Zr. The horizontal axis is the RD for all images. Alpha and beta indicate each phase, respectively.
Abbreviations: SEM, scanning electron microscopy; WR, warm-rolled; HR, hot-rolled; EBSD, electron backscatter diffraction; RD, rolling direction.

equiaxed grains (d=0.3 μm) were formed. This suggests that the submicrocrystalline structure has been formed by the warm-rolling process of Ti-13Nb-13Zr. In contrast, the HR alloy exhibited a typical coarse lamellar structure and elongated grains, of which the thickness was measured to be 0.5 μm. It is obvious that its actual grain size is significantly larger compared to that of the WR Ti-13Nb-13Zr. Figure 2 demonstrates the XRD results revealing the (α+β) structure for both alloys, which is in good accord with the EBSD results. The martensitic transformation would be suppressed due to the diffusion of niobium atoms into the β phase.[11] It is interesting from the XRD data that the alloys demonstrated the different texture behaviors. The WR plane normal to the RD exhibited the strong (110)β peak. Such a texture development is typically observed in caliber-rolled body-centered cubic alloys.[13] The (0002)α and (10-12)α peaks

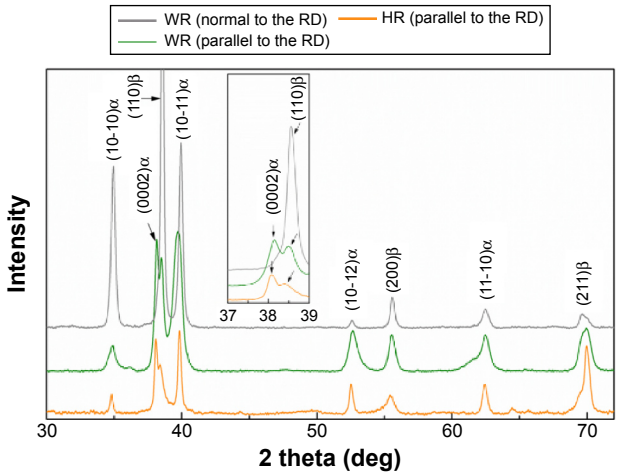

Figure 2 XRD line profiles of the WR and HR Ti-13Nb-13Zr.
Note: The inset is the magnified image ranging from 37° to 39°.
Abbreviations: XRD, X-ray diffraction; WR, warm-rolled; HR, hot-rolled; RD, rolling direction.

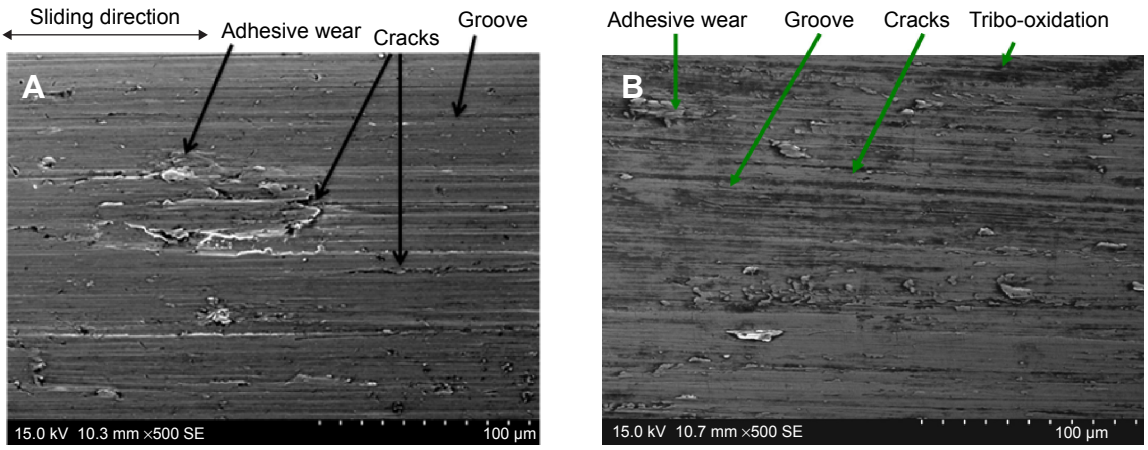

Figure 3 SEM micrograph of wear tracks.
Notes: (**A**) WR and (**B**) HR Ti-13Nb-13Zr.
Abbreviations: SEM, scanning electron microscopy; WR, warm-rolled; HR, hot-rolled.

were significantly weak in this plane in contrast to the planes parallel to the RD. This type of texture can be observed in pure titanium and interpreted in terms of slip/twin behavior in a hexagonal close-packed system.[14,15]

It is noted that the WR Ti-13Nb-13Zr exhibited the superior tensile properties in comparison to other forms of Ti-13Nb-13Zr alloy as discussed in our previous work; the WR alloy exhibited a tensile stress of 1,050 MPa, while both HR alloy and ASTM Ti-13Nb-13Zr possessed the value of 850 MPa.[16,17] Moreover, the WR alloy exhibited the higher hardness (HV 335±5) than the HR alloy (HV 215±4) as well as the solution-treated and cold-rolled sample (HV 285±7).[18] This is understood by the conclusion that Ti-13Nb-13Zr exhibits a higher hardness when it consists of the finer microstructural features.[19] These results prove the great improvement in mechanical properties via the warm-rolling process.

The friction coefficient of WR and HR alloys was measured to be around 0.42–0.45, which was similar to the values reported in the literature.[18,20] The wear rate was determined by the expression, $WR = (V \times S \times N \times f)/L$ where V is the volume loss, S =15 mm is the stroke length, N =30,000 is the number of cycles, f =2 Hz is the frequency, and L =10 N is the applied load. The results presented no significant variation between the WR (1.05×10^{-5} mm^3/Nm) and HR Ti-13Nb-13Zr (4.44×10^{-5} mm^3/Nm). In other words, no straightforward relationship was confirmed between hardness and wear properties in the investigated materials, as also supported by previous works.[10,21] Figure 3 presents worn scars produced during the wear sliding, suggesting that the abrasive wear is dominant in both Ti-13Nb-13Zr alloys. Moreover, the tribocorrosion also occurred in the HR Ti-13Nb-13Zr as evidenced by the formation of dark patches observed in Figure 3B; the WR alloy did not show such a microstructural characteristic.

Figure 4 provides polarization curves of the WR and HR Ti-13Nb-13Zr where the WR alloy was evaluated in two planes to investigate a texture effect on corrosion behavior. The planes parallel to the RD exhibited the stable passivation up to 1,200 mV, while the WR alloy plane normal to the RD presented the formation of thick oxide layer above 1,200 mV. The specific corrosion data are summarized in Table 1. It should be noted that both WR planes exhibited the lower corrosion current densities (1.11 µA/cm^2 for plane normal to the RD and 1.33 µA/cm^2 for plane parallel to the RD) compared to the HR alloy (1.71 µA/cm^2). The corrosion current density is directly proportional to the corrosion rate,[22] indicating the better corrosion resistance of the WR alloy. These results explain the fact that only the HR alloy exhibited the tribocorrosion after the wear test, because

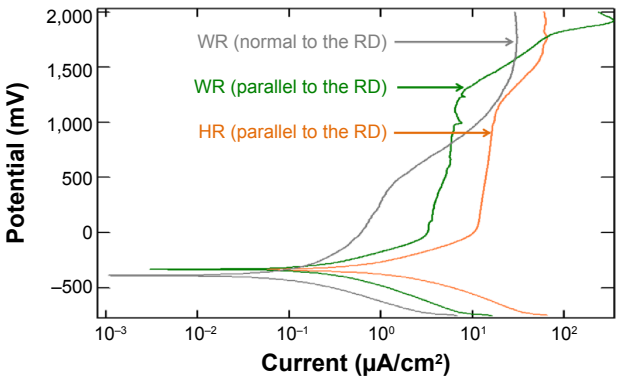

Figure 4 Potentiodynamic curves measured in Hank's solution for the investigated Ti-13Nb-13Zr alloys.
Abbreviations: WR, warm-rolled; HR, hot-rolled; RD, rolling direction.

Table 1 Results of potentiodynamic polarization tests

Material	E_{corr} (mV)	I_{corr} (μA/cm²)	R_p (Ohm·cm²)	I_{pass} (μA/cm²)
WR (normal to the RD)	–332.06	1.11	25.64	1.6
WR (parallel to the RD)	–284.84	1.31	53.67	5.7
HR (parallel to the RD)	–232.36	1.71	47.15	11.2

Abbreviations: WR, warm-rolled; HR, hot-rolled; RD, rolling direction; E_{corr}, corrosion potential; I_{corr}, corrosion current density; R_p, polarization resistance; I_{pass}, passivation current density.

the alloy was more prone to the corrosion in the simulated body fluid.

Corrosion resistance is influenced by various factors such as chemical composition, surface roughness, grain size, and texture.[5,10,23] It is reasonable that the grain size and texture mainly contributed to the corrosion behavior in this work as the first two factors were comparable among the investigated materials. The enhanced corrosion resistance of WR alloy is attributed to its submicrocrystalline structure (ie, ultrafine grains); the grain refinement is beneficial to corrosion resistance in case of Ti-13Nb-13Zr, although it is not applicable to other metals.[10] Such an improvement would be achieved by the formation of stable oxide layers on the surface composed of a considerable amount of grain boundaries.[24] The different corrosion behaviors depending on the plane of WR alloy originate from the variation in developed texture. The (110) plane is one of the crystallographic groups having the highest atomic density in the body-centered cubic structure.[25] It is of particular interest that corrosion resistance increases with increasing atomic density of crystallographic plane,[23] which rationalizes the lowest corrosion current density of WR plane normal to the RD with the strong (110)β texture.

Conclusion

The WR Ti-13Nb-13Zr demonstrated a submicrocrystalline structure formed by the warm-rolling process, which provided a significant increase in hardness and tensile stress compared to the HR alloy composed of coarse elongated grains. Although there was no notable difference in wear resistance between the two alloys, the WR Ti-13Nb-13Zr exhibited a better resistance to corrosion in the simulated body fluid conditions. The improvement was attributed to the submicrocrystalline structure with atomically dense crystallographic plane developed by the warm-rolling. The present study confirmed the enormous potential of WR Ti-13Nb-13Zr with not only great mechanical properties but also high corrosion resistance in the simulated body fluid.

Acknowledgment

The authors would like to thank Dr Fathima Zivic for her technical support.

Disclosure

The authors have no conflicts of interest to disclose.

References

1. Davidson JA, Mishra AK, Kovacs P, Poggie RA. New surface-hardened, low-modulus, corrosion-resistant Ti13Nb13Zr alloy for total hip arthroplasty. *Biomed Mater Eng*. 1994;4(3):231–243.
2. Long M, Rack HJ. Titanium alloys in total joint replacement – a materials science perspective. *Biomater*. 1998;19(18):1621–1639.
3. Geetha M, Singh AK, Asokamani R, Gogia AK. Ti based biomaterials, the ultimate choice for orthopaedic implants – A review. *Progress in Materials Science*. 2009;54(3):397–425.
4. Budinski KG. Tribological properties of titanium alloys. *Wear*. 1991; 151(2):203–217.
5. Geetha M, Kamachi Mudali U, Gogia AK, Asokamani R, Raj B. Influence of microstructure and alloying elements on corrosion behavior of Ti–13Nb–13Zr alloy. *Corrosion Science*. 2004;46(4):877–892.
6. Lee YT. Titanium. *Seoul: Korea Metal Journal*. 2009.
7. Lee T, Nakai M, Niinomi M, Park CH, Lee CS. Phase transformation and its effect on mechanical characteristics in warm-deformed Ti-29Nb-13Ta-4.6Zr alloy. *Metals and Materials International*. 2015;21(1): 202–207.
8. Zardiackas LD, Kraay MJ, Freese HL, editors. *Titanium, Niobium, Zirconium, and Tantalum for Medical and Surgical Applications*. ASTM; 2006.
9. Schneider SG, Nunes CA, Rogero SO, Higa OZ, Bressiani JC. Mechanical properties and cytotoxic evaluation of the Ti-13Nb-13Zr alloy. *Biomecánica*. 2000;8(1):84–87.
10. Suresh KS, Geetha M, Richard C, et al. Effect of equal channel angular extrusion on wear and corrosion behavior of the orthopedic Ti–13Nb–13Zr alloy in simulated body fluid. *Materials Science and Engineering: C*. 2012;32(4):763–771.
11. Lee T, Heo YU, Lee CS. Microstructure tailoring to enhance strength and ductility in Ti–13Nb–13Zr for biomedical applications. *Scripta Materialia*. 2013;69(11–12):785–788.
12. Park CH, Park JW, Yeom JT, Chun YS, Lee CS. Enhanced mechanical compatibility of submicrocrystalline Ti-13Nb-13Zr alloy. *Materials Science and Engineering: A*. 2010;527(18–19):4914–4919.
13. Inoue T, Yin F, Kimura Y, Tsuzaki K, Ochiai S. Delamination Effect on Impact Properties of Ultrafine-Grained Low-Carbon Steel Processed by Warm Caliber Rolling. *Metallurgical and Materials Transactions A*. 2010;41(2):341–355.
14. Wagner F, Bozzolo N, Van Landuyt O, Grosdidier T. Evolution of recrystallisation texture and microstructure in low alloyed titanium sheets. *Acta Materialia*. 2002;50(5):1245–1259.
15. Chun YB, Yu SH, Semiatin SL, Hwang SK. Effect of deformation twinning on microstructure and texture evolution during cold rolling of CP-titanium. *Materials Science and Engineering: A*. 2005; 398(1–2):209–219.
16. ASTM. F1713-08. *Standard Specification for Wrought Titanium-13Niobium-13Zirconium Alloy for Surgical Implant Applications*. West Conshohocken, PA: ASTM International; 2013.
17. Jung HS, Lee T, Kwon IK, Kim HS, Hahn SK, Lee CS. Surface modification of multi-pass caliber-rolled Ti alloy with dexamethasone-loaded graphene for dental applications. *ACS Appl Mater Interfaces*. 2015;7(18):9598–9607.

18. Cvijović-Alagić I, Cvijović Z, Mitrović S, Rakin M, Veljović Đ, Babić M. Tribological Behaviour of Orthopaedic Ti-13Nb-13Zr and Ti-6Al-4V Alloys. *Tribology Letters*. 2010;40(1):59–70.
19. Geetha M, Singh AK, Muraleedharan K, Gogia AK, Asokamani R. Effect of thermomechanical processing on microstructure of a Ti–13Nb–13Zr alloy. *Journal of Alloys and Compounds*. 2001;329(1–2):264–271.
20. Durgalakshmi D, Chandran M, Manivasagam G, Ramachandra Rao MS, Asokamani R. Studies on corrosion and wear behavior of submicrometric diamond coated Ti alloys. *Tribology International*. 2013;63:132–140.
21. Majumdar P, Singh SB, Chakraborty M. Wear response of heat-treated Ti–13Zr–13Nb alloy in dry condition and simulated body fluid. *Wear*. 2008;264(11–12):1015–1025.
22. Songür M, Çelikkan H, Gökmeşe F, Şimşek SA, Altun NŞ, Aksu ML. Electrochemical corrosion properties of metal alloys used in orthopaedic implants. *Journal of Applied Electrochemistry*. 2009;39(8):1259–1265.
23. Hoseini M, Shahryari A, Omanovic S, Szpunar JA. Comparative effect of grain size and texture on the corrosion behaviour of commercially pure titanium processed by equal channel angular pressing. *Corrosion Science*. 2009;51(12):3064–3067.
24. Gurao NP, Manivasagam G, Govindaraj P, Asokamani R, Suwas S. Effect of Texture and Grain Size on Bio-Corrosion Response of Ultrafine-Grained Titanium. *Metallurgical Materials Transactions A*. 2013;44(12):5602–5610.
25. Dieter GE. *Mechanical Metallurgy*. SI Metric Edition. London: McGraw-Hill; 1988.